

## ARTICLES

**High-Quality Alloyed CdS<sub>x</sub>Se<sub>1-x</sub> Whiskers as Waveguides with Tunable Stimulated Emission**

Anlian Pan,<sup>\*,†,‡</sup> Ruibin Liu,<sup>†,‡</sup> Feifei Wang,<sup>†,‡</sup> Sishen Xie,<sup>‡</sup> Bingsuo Zou,<sup>\*,†,‡</sup>  
Margit Zacharias,<sup>§</sup> and Zhong Lin Wang<sup>||</sup>

Micro-Nano Technologies Research Center, Hunan University, Changsha, 410082 P.R. China, Institute of Physics, Chinese Academy of Sciences, Beijing, 100080 P.R. China, MPI of Microstructure Physics, Weinberg 2, Halle 06120, Germany, and School of Materials Science and Engineering, Georgia Institute of Technology, Atlanta, Georgia 30332-0245

Received: July 22, 2006; In Final Form: September 5, 2006

High-quality ultra-long alloyed CdS<sub>x</sub>Se<sub>1-x</sub> ( $0 \leq x \leq 1$ ) whiskers were obtained by a simple thermal evaporation route. The near band-edge emission in these whiskers can be effectively guided at the sub-millimeter scale under continuous-wave laser excitation. As good optical waveguide cavities, the whiskers exhibit stimulated emissions under pulsed light excitation at room temperature for all compositions  $0 \leq x \leq 1$ . The spectral positions of the sharp emission lines of the whiskers were tuned by their compositions, covering the spectral range from green to red.

**1. Introduction**

One-dimensional (1D) structured semiconductor nanowires or whiskers have many special properties arising from quantum or photon confinement and have wide potential applications in light emitting diodes, lasers, sensors, waveguides, and photo-detectors.<sup>1–10</sup> They are also attractive for building blocks or assembling elements of integrated small systems since these individual structures can function as both device elements and interconnects.<sup>11–13</sup> More importantly, 1D wide-band semiconductor nanostructures have been shown to function as waveguide cavities and can give stimulated emission or lasing under high-intensity excitation, and thus can be used as nanolasers. For example, ZnO, GaN, and ZnS nanowires and/or nanobelts can be used as near-ultraviolet (UV) nanolasers,<sup>14–16</sup> and 1D CdS nanostructures can serve as green light nanolasers.<sup>17</sup> However, the lasing wavelength and hence the color of these nanolasers based on binary semiconductors can hardly be tuned, which restricts their wide applications in biology imaging, fluorescence labeling, light telecommunication, surgery, and small lighting devices. Research on 1D ternary or multielement alloyed semiconductors is expected to be important because their band gaps and thus their emission wavelengths can be modulated by their compositions.<sup>18–25</sup>

Ternary CdSSe alloy is an important semiconductor and has a wide range of potential applications based on its excellent properties such as large nonlinear susceptibilities, good photo-conduction, and fast response times, and its band gap between  $\sim 2.44$  eV (for CdS) and  $\sim 1.72$  eV (for CdSe) can be tuned by

the sulfur-to-selenium ratio in the visible range.<sup>22–25</sup> In particular, CdSSe is also a very good laser media and can be used to produce lasing in the visible spectral region. Electron-beam pumped or optically pumped CdSSe platelet lasers were reported several decades ago.<sup>26–28</sup> Lu et al. found that CdSSe quantum dots in glass spherical microcavity can also give efficient multimode lasing.<sup>29</sup> Recently, we first reported high-quality shearlike CdS<sub>x</sub>Se<sub>1-x</sub> nanobelts fabricated by a one-step thermal-evaporation process, and realized the color-tunable photoluminescence (PL) covering the visible spectral region.<sup>23</sup> However, such shearlike CdSSe structures cannot be efficient optical waveguide cavities because of their nonuniform figuration. In this paper, we develop a multistep thermal-evaporation route to get high-quality and highly uniform CdS<sub>x</sub>Se<sub>1-x</sub> ( $0 < x < 1$ ) whiskers. The PL investigations indicate that these CdSSe whiskers can act as promising multicolor waveguides and can realize color-tunable stimulated emissions in the spectral range from green to red.

**2. Experimental Section**

CdSSe whiskers were synthesized by a multistep physical evaporation route. Appropriate amounts of commercial-grade CdS and CdSe powders were placed onto a ceramic plate at the center of a quartz tube, which was placed into a horizontal tube furnace. Next to the ceramic plate, several pieces of silicon slices coated with 10 nm Au film were placed downstream of the gas flow. Prior to heating, high-purity He was injected into the quartz tube with a constant flowing rate ( $\sim 20$  sccm) to eliminate the O<sub>2</sub> inside. After 60 min, the flowing rate of the carrier He gas was adjusted to  $\sim 1$  sccm, and the furnace was rapidly heated to 850 °C and maintained for about 120 min without changing the conditions. Then, CdSSe whiskers were obtained from the surface of the silicon slice with the substrate temperature of  $\sim 700$  °C. The composition of the whiskers was

\* Authors to whom correspondence should be addressed. E-mail: zoubs@aphy.iphy.ac.cn (B.Z); pananlian@aphy.iphy.ac.cn (A.P.).

<sup>†</sup> Hunan University.

<sup>‡</sup> Chinese Academy of Sciences.

<sup>§</sup> MPI of Microstructure Physics.

<sup>||</sup> Georgia Institute of Technology.

tuned by changing the molar ratio of the CdS and CdSe powder in the evaporation source.

Scanning electron microscope (SEM) images and the energy dispersive spectroscopy (EDS) were achieved on a Hitachi S-4200 microscope. The transmission electron microscope (TEM) observations were carried out on a Hitachi H-800 microscope with an accelerating voltage of 200 kV. X-ray powder diffraction (XRD) experiments were done using a Japan Rigaku D/max-2400 X-ray diffractometer equipped with graphite-monochromatized Cu K $\alpha$  radiation ( $\lambda = 1.54178 \text{ \AA}$ ). Optical waveguide properties were investigated using a commercial scanning near-field optical microscope (NSOM) from RHK Technology (U.S.A.). During the experiment, the continuous wave laser beam (He–Cd, 442 nm; power, 10 mW) was focused and illuminated at the center of an examined single CdSSe whisker which was predispersed on a silicon substrate coated with a 500 nm thick thermally grown SiO<sub>2</sub> layer. A color CCD through an objective lens was used for collecting the far-field optical image of the excited whiskers. Stimulated emission measurements of single CdSSe whiskers were conducted using the third harmonic of a Nd:YAG laser (355 nm; spot size,  $\sim 0.5 \text{ mm}^2$ ) with pulse width 6 ns as the excitation source. The PL was detected by a spectrometer (Acton Research Corp. Spectra Pro 500i) equipped with a liquid N<sub>2</sub>-cooled charge coupled device (CCD) camera (Roper Scientific), with an expected spectral resolution of  $\sim 0.2 \text{ nm}$ .

### 3. Results and Discussion

The morphology and the composition of the obtained CdSSe samples are controlled and strongly affected by the flow rate of the carrier gas, the molar ratio of the source powder, the source temperature, and the substrate temperature (or the substrate distance from the source). As reported in ref 23, when the flow rate and the source temperature are 20 sccm and 900 °C, respectively, shearlike CdS<sub>*x*</sub>Se<sub>1-*x*</sub> nanobelts with continuously tuned compositions ( $0 < x < 1$ ) can be simultaneously obtained from the silicon substrates at different deposition temperatures (650–800 °C), using equal molar CdS and CdSe in the source powder. Further investigations indicate that the morphology of the obtained CdSSe sample at a fixed substrate is also highly dependent on the carrier gas flow rate, the temperature of the evaporation source, and the reaction time. When the flow rate and the source temperature are decreased to 1 sccm and 850 °C, respectively, and the reaction time is long enough ( $> 100 \text{ min}$ ), then ultralong and uniform CdSSe whiskers can always be obtained from the silicon substrate at a temperature of  $\sim 700 \text{ °C}$ , whatever the molar ratio of CdS and CdSe in the source powder. Then, under the above growth condition, CdSSe whiskers with different composition can be obtained just by tuning the molar ratio of the evaporation source. That is to say, with other reaction parameters unchanged, the compositions of the obtained whiskers at a same deposition temperature or position are well defined by the molar ratio CdS/CdSe of the source powder.

Figure 1a shows the locally amplified scanning electron microscope (SEM) image of a representative CdSSe whisker sample, which indicates that most of the whiskers are straight with a uniform width of several micrometers and their length can be extended to more than several hundreds of micrometers. The enlargement of a representative single CdSSe whisker (see the inset of Figure 1a) shows that the whiskers have very clean and uniform surfaces with a rectangle cross section of  $\sim 600 \text{ nm} \times 5 \text{ }\mu\text{m}$  in size. The in-situ energy-dispersive X-ray analysis (EDX) (Figure 1b) proves that the whiskers contain the elements

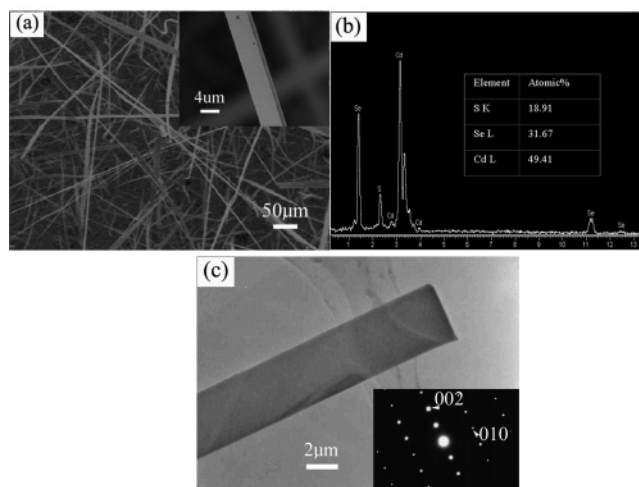


**Figure 1.** (a) Locally amplified SEM image of a representative CdSSe whisker. Inset shows the enlargement of a representative single CdSSe whisker. (b) The in-situ energy-dispersive X-ray spectrum of the whiskers. (c) The local TEM image of a representative single whisker and its corresponding selected area electron diffraction pattern (inset).

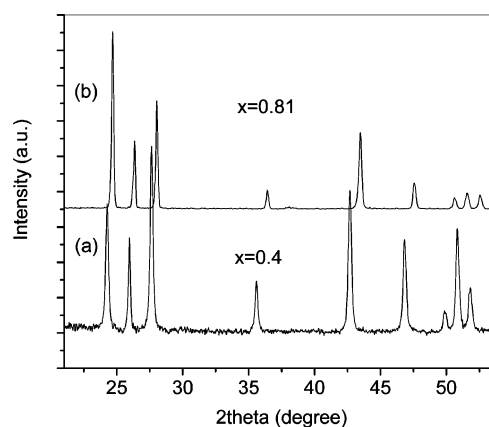


**Figure 2.** Normalized XRD pattern of two representative CdSSe whiskers (CdS<sub>0.4</sub>Se<sub>0.6</sub> and CdS<sub>0.81</sub>Se<sub>0.19</sub>).

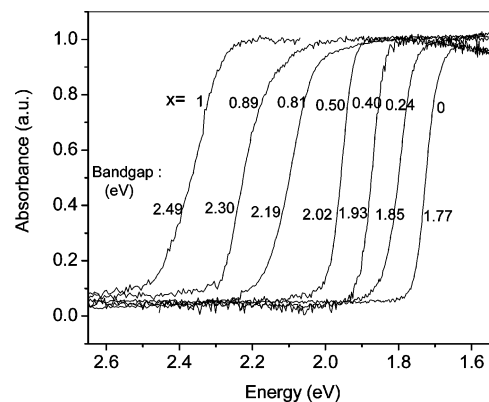


**Figure 3.** UV-vis reflectance spectra of the obtained CdS<sub>*x*</sub>Se<sub>1-*x*</sub> ( $0 \leq x \leq 1$ ) whiskers.

S, Se, and Cd. The atomic ratio of (S + Se)/Cd is very close to 1 (see the inset of this image), indicating the formation of ternary CdSSe. Moreover, the compositions (molar ratio S/Se) along all the single whiskers from a same silicon substrate have very minor differences, which can be further demonstrated by the very steep absorption edge in the UV-vis reflectance spectra (see Figure 3).

Figure 1c shows the transmission electron microscopy (TEM) image of a representative single whisker, which demonstrates

**TABLE 1: Composition and Band Gap Values of the Obtained CdSSe Whiskers with the Mixed CdS/CdSe Powder of Different Molar Ratios as the Reaction Source**

molar ratio (CdS:CdSe) compositions of CdS <sub>x</sub> Se <sub>1-x</sub> whiskers (x)	100:0	85:15	75:25	50:50	35:65	20:80	0:100
compositions of CdS <sub>x</sub> Se <sub>1-x</sub> whiskers (x)	1.0	0.89	0.81	0.50	0.40	0.24	0
band gap (eV)	2.49	2.30	2.19	2.02	1.93	1.85	1.77

that the whiskers have sharp cleaved end facets, coming from the sonication process used to take the whiskers off the silicon substrate. The selected area electron diffraction pattern (inset of Figure 1c) confirms the single-crystal quality of the whiskers and can be indexed to have a hexagonal structure with lattice parameters  $a = 0.418$  nm and  $c = 0.678$  nm with the growth along the [010] direction.

The composition and the crystallographic phase of the whiskers were obtained by X-ray powder diffraction (XRD). Figure 2 shows the normalized XRD pattern of two representative CdSSe whisker samples. All diffraction peaks in each sample can be indexed to the typical hexagonal wurtzite crystals, with the peak positions located somewhere between those of bulk wurtzite CdS (JCPDS 41-1049) and CdSe (JCPDS 77-2309). According to Vegard's law for ternary alloys<sup>24</sup> and using the lattice parameters deduced from the XRD results, the compositions of the whiskers shown in Figure 2a,b can be determined as CdS<sub>0.4</sub>Se<sub>0.6</sub> and CdS<sub>0.81</sub>Se<sub>0.19</sub>, respectively, which is in agreement with the data from EDS examination. These results reveal that the obtained whiskers are wurtzite structured CdSSe alloys. Table 1 gives the compositions of the obtained whiskers with the mixed CdS/CdSe powder of different molar ratios as the reaction source.

To demonstrate that the band gap of the ternary CdSSe whiskers can be well tuned by their compositions, we measured the UV-vis reflectance spectra of the obtained CdS<sub>x</sub>Se<sub>1-x</sub> samples. From Figure 3, one can clearly see that all samples exhibit a very steep absorption edge in their respective spectra, but the spectral position of the edge continuously blue shifts with an increase of the composition  $x$  (S ratio) in the whiskers, which is in good agreement with the results of CdSSe films and nanowires.<sup>24,30</sup> Using the reflectance data and adopt the well-known relation of  $(ah\nu)^2$  versus the photon energy  $h\nu$ ,<sup>31</sup> the band gap values of the whiskers were calculated, which are also listed in Table 1, too. The above results further show that the obtained CdS<sub>x</sub>Se<sub>1-x</sub> ( $0 < x < 1$ ) whiskers are well-crystallized ternary alloys.

Figure 4a shows the far-field image of a representative single CdSSe whisker, and Figure 4b is its corresponding emission image under the excitation of a beam of focused laser, with a separation of about 80  $\mu\text{m}$  between the excitation spot and the upper end of the whisker. The big bright spot in the lower left of Figure 4b is the in-situ PL under laser excitation, part of which was guided through the whisker and emitted at its ends (see the upper right spot of Figure 4b). It is very clear that the guided light primarily is emitted at the tip of the whisker, with a relatively weak emission in other regions. Figure 4c represents the corresponding emission image when the excitation spot was about 500  $\mu\text{m}$  away from the upper end of the whisker, which still shows clearly the emission of the guided light at its end. Further investigations indicate that all the obtained uniform whiskers, with the transverse sizes larger than 100 nm but not much larger than  $2\lambda$  ( $\lambda$ , the wavelength of propagating light) and with the length larger than 10  $\mu\text{m}$ , have a similar waveguide effect, since they are highly crystallized and are highly optically confined in transverse directions. These results demonstrate that the obtained whiskers are good optical waveguide cavities.

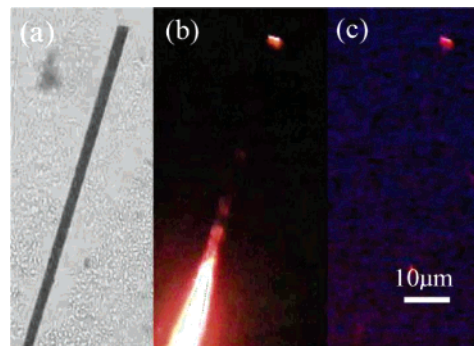


**Figure 4.** (a, b) Far-field image of a representative single CdSSe whisker and its corresponding emission images, respectively, when it was excited by a focused laser (442 nm), with the spatial separation between the excitation spot and the upper end of the whisker around 80  $\mu\text{m}$ , and (c) the corresponding emission image when the spatial separation was about 500  $\mu\text{m}$ .

From the above discussion, the CdSSe whiskers can act as good optical waveguide media and have sharp cleaved end facets after sonication processing, which make them suitable as Farby-Perot (F-P) cavities to realize stimulated emission or lasing. Figure 5a shows the power-dependent PL spectra of a representative CdS<sub>0.4</sub>Se<sub>0.6</sub> whisker excited by the nanosecond pulses (Nd:YAG, 355 nm) at room temperature. At low excitation intensities, a broad emission band appears at  $\sim 650$  nm, which is attributed to the spontaneous radiative transition of the CdS<sub>0.4</sub>Se<sub>0.6</sub> whisker at the band edge. This agrees well with the band-edge energy calculated from the relationship between the PL emission energy and the composition of CdSSe alloy films.<sup>24</sup> With increasing excitation power, the emission intensity increases, accompanied by a narrowing of the emission band. When the excitation density becomes above  $\sim 35$  kW/cm<sup>2</sup>, an ultranarrow peak (lasing mode) appears superimposed on the main band. The upper right of Figure 5a shows the excitation power-dependent emission intensities and line widths of the PL band of the CdS<sub>0.4</sub>Se<sub>0.6</sub> whisker. The peak emission intensities show a clear superlinear dependence on the excitation power with a threshold power of  $\sim 35$  kW/cm<sup>2</sup>. At the same time, the full width at half-maximum (fwhm) decreases with the power, and has a sharp fall-off at around the threshold. The band narrowing and the superlinear increment of emission intensity above the threshold indicate the occurrence of stimulated emission and lasing in the CdS<sub>0.4</sub>Se<sub>0.6</sub> whisker.<sup>3</sup> Figure 5b shows the power-dependent PL spectra of one representative CdS<sub>0.81</sub>Se<sub>0.19</sub> whisker, and its upper right inset gives the corresponding power-dependent emission intensities and line widths of the PL bands. Apparently, the superlinear increment of emission intensity with the excitation power and the appearance of supernarrow emission modes demonstrate that the CdS<sub>0.81</sub>Se<sub>0.19</sub> whiskers can also realize stimulated emission under high-intensity excitation, with a threshold power of around 50 kW/cm<sup>2</sup>. Further PL investigations indicate that the CdS<sub>x</sub>Se<sub>1-x</sub> whiskers with other compositions can all realize stimulated emission under high power excitation. Figure 5c compares the representative PL spectra of single CdS<sub>x</sub>Se<sub>1-x</sub> whiskers of varied composition  $0 \leq x \leq 1$  (see the inset for the corresponding  $x$  value) under excitation above their corresponding excitation thresholds (see the inset of Figure 5c), all of which exhibit ultranarrow lasing modes. Furthermore, the spectral position of these ultranarrow lasing lines can be continuously tuned by the composition, covering the spectral range from green to red.

The lasing thresholds for the CdS, CdS<sub>0.89</sub>Se<sub>0.11</sub>, CdS<sub>0.81</sub>Se<sub>0.19</sub>, CdS<sub>0.5</sub>Se<sub>0.5</sub>, CdS<sub>0.4</sub>Se<sub>0.6</sub>, CdS<sub>0.24</sub>Se<sub>0.76</sub>, and CdSe whiskers are included in Figure 5c, respectively. It is clear that the thresholds

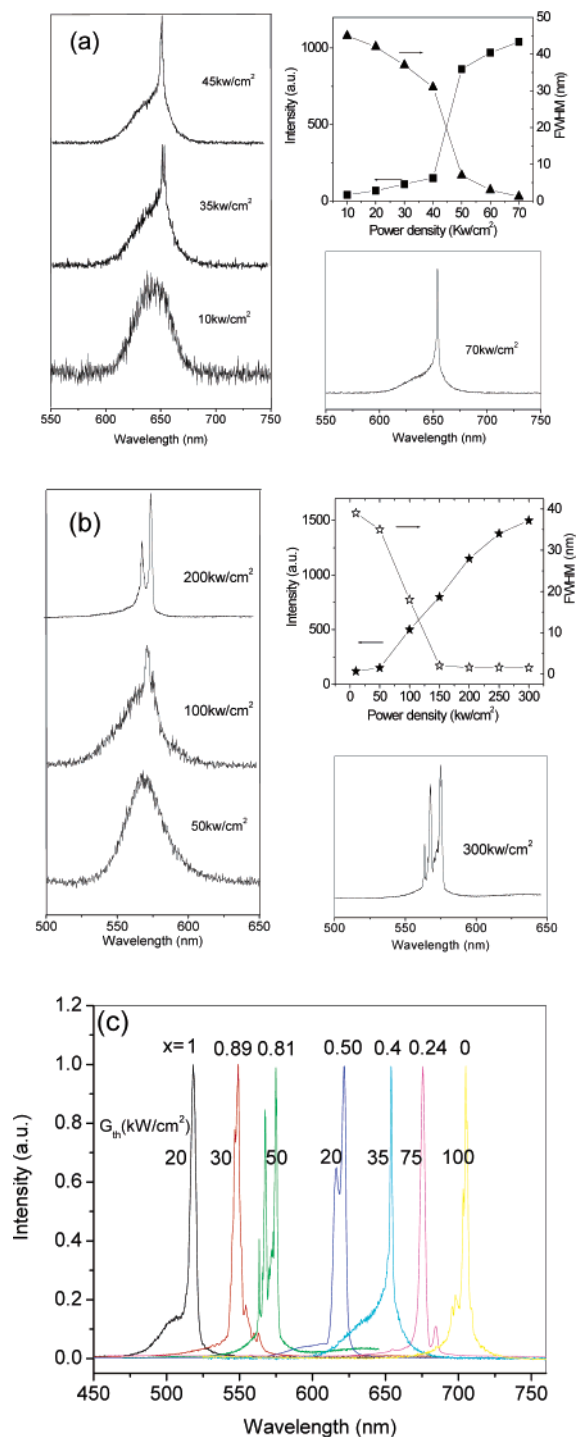


**Figure 5.** (a) Power-dependent PL spectra of  $\text{CdS}_{0.4}\text{Se}_{0.6}$  whiskers excited by the nanosecond pulse (355 nm) and the excitation power-dependent emission intensity and line width of the PL bands (the upper-right inset). (b) Power-dependent PL spectra of the  $\text{CdS}_{0.81}\text{Se}_{0.19}$  whiskers, and their corresponding excitation power-dependent emission intensity and line width (the upper-right inset). (c) Representative PL spectra of the  $\text{CdS}_x\text{Se}_{1-x}$  whiskers with varied composition under excitation above the threshold power.

of the ternary  $\text{CdS}_x\text{Se}_{1-x}$  ( $0 < x < 1$ ) whiskers are similar to that of the binary CdS or CdSe compound, and are also comparable to those of some other high-quality 1D semiconductor nanostructures.<sup>15,16</sup> It is believed that the lasing threshold value is a function of both material quality and optical-cavity quality,<sup>18</sup> and the threshold of ternary compound is usually significantly higher than that of the corresponding binary compounds, resulting from its very often poor crystalline quality.

Since no clear differences in the optical-cavity quality of our different  $\text{CdS}_x\text{Se}_{1-x}$  ( $0 \leq x \leq 1$ ) whiskers were detected, the ternary alloy structures showing lasing properties as good as CdS and CdSe should mainly come from their high-quality crystallization.<sup>28</sup> In addition, the thresholds of all of the 1D CdSSe whiskers are much lower than those of platelet lasers and quantum dots in a glass spherical microcavity.<sup>28,29</sup> The very low threshold can mainly be attributed to two aspects. On one hand, compared to the quantum dots dispersed in a microcavity, the whiskers not only have high optical confinement at the radial directions, but also have continuous gain media along the long axis, which results in very larger carrier density under pulsed light excitation and might greatly decrease the lasing threshold. On the other hand, the whiskers themselves are natural lasing cavities, and the length of a single whisker is the F–P cavity length  $L$ . According to ref 32, the threshold of such an F–P cavity is inversely proportional to the cavity length ( $L$ ) by  $G_{th} \sim (1/2L)\ln(1/R_1R_2)$ , where  $R_1$  and  $R_2$  are the end facet reflections. The  $L$  value of the CdSSe whiskers (several hundreds of microns) is much larger than that of the reported platelet lasers (several tens of microns),<sup>28</sup> which also lead to the former having a lower threshold than the latter.

#### 4. Conclusion

In summary, single-crystal ultralong alloyed  $\text{CdS}_x\text{Se}_{1-x}$  ( $0 \leq x \leq 1$ ) whiskers were fabricated by a Au-catalyzed thermal evaporation route. Most of the whiskers have uniform rectangle cross sections with widths of several micrometers and depths of several hundreds of nanometers. These ultralong  $\text{CdS}_x\text{Se}_{1-x}$  whiskers are good optical waveguides at the sub-millimeter scale. Stimulated emissions were observed in the whiskers of varied composition  $0 \leq x \leq 1$  under pulsed light excitation at room temperature. This finding indicates that the  $\text{CdS}_x\text{Se}_{1-x}$  whiskers have potential applications in adjustable nano/micro lasers.

**Acknowledgment.** The authors are grateful for the financial support of National 973 Project (2002CB713802), Nanospecific projects (9046024 and key) of NSFC of China, project (grant 705040) of MOE of China, and 985 project of HNU.

#### References and Notes

- (1) Hu, J.; Ouyang, M.; Yang, P.; Lieber, C. M. *Nature (London)* **1999**, *399*, 48.
- (2) Duan, X. F.; Huang, Y.; Agarwal, R.; Lieber, C. M. *Nature (London)* **2003**, *421*, 241.
- (3) Ding, J. X.; Zapfen, J. A.; Chen, W. W.; Lifshitz, Y.; Lee, S. T.; Meng, X. M. *Appl. Phys. Lett.* **2004**, *85*, 2361.
- (4) Cui, Y.; Wei, Q.; Park, H.; Lieber, C. M. *Science* **2001**, *293*, 1289.
- (5) Li, C.; Zhang, D.; Liu, X.; Han, S.; Tang, T.; Han, J.; Zhou, C. *Appl. Phys. Lett.* **2003**, *82*, 1613.
- (6) Law, M.; Sirbully, D. J.; Johnson, J. C.; Goldberger, J.; Saykally, R. J.; Yang, P. *Science* **2004**, *305*, 1269.
- (7) Barrelet, C. J.; Greytak, A. B.; Lieber, C. M. *Nano Lett.* **2004**, *4*, 1981.
- (8) Pan, A.; Liu, D.; Liu, R.; Wang, F.; Zou, B. *Small* **2005**, *1*, 980.
- (9) Wang, J.; Gudiksen, M. S.; Duan, X.; Cui, Y.; Lieber, C. M. *Science* **2001**, *293*, 1455.
- (10) Kind, H.; Yan, H.; Messer, B.; Law, M.; Yang, P. *Adv. Mater.* **2002**, *14*, 158.
- (11) Huang, Y.; Duan, X.; Lieber, C. M. *Small* **2005**, *1*, 142.
- (12) Hu, J.; Odom, T. W.; Lieber, C. M. *Acc. Chem. Res.* **1999**, *32*, 435.
- (13) Cui, Y.; Duan, X.; Huang, Y.; Lieber, C. M. In *Nanowires and Nanobelts—Materials, Properties and Devices*; Wang, Z. L., Ed.; Kluwer Academic/Plenum Publishers: Dordrecht, 2003; pp 3–68.
- (14) Huang, M. H.; Mao, S.; Feick, H.; Yan, H.; Wu, Y.; Kind, H.; Weber, E.; Russo, R.; Yang, P. *Science* **2001**, *292*, 1897.
- (15) Gradečak, S.; Qian, F.; Li, Y.; Park, H. G.; Lieber, C. M. *Appl. Phys. Lett.* **2005**, *87*, 173111.

- (16) Zapien, J. A.; Jiang, Y.; Meng, X. M.; Chen, W.; Au, F. C. K.; Lifshitz, Y.; Lee, S. T. *Appl. Phys. Lett.* **2003**, *84*, 1189.
- (17) (a) Pan, A. L.; Liu, R.; Yang, Q.; Zhu, Y.; Yang, G.; Zou, B. S.; Chen, K. *J. Phys. Chem. B* **2005**, *109*, 24268. (b) Pan, A. L.; Liu, R.; Zou, B. S. *Appl. Phys. Lett.* **2006**, *88*, 173102.
- (18) Liu, Y.; Zapien, J. A.; Shan, Y. Y.; Geng, C. Y.; Lee, C. S.; Lee, S. T. *Adv. Mater.* **2005**, *17*, 1372.
- (19) Zhong, X.; Feng, Y.; Knoll, W.; Han, M. *J. Am. Chem. Soc.* **2003**, *125*, 13559.
- (20) Bailey, R. E.; Nie, S. *J. Am. Chem. Soc.* **2003**, *125*, 7100.
- (21) Petrov, D. V.; Santos, B. S.; Pereira, G. A. L.; Donega, C. D. M. *J. Phys. Chem. B* **2002**, *106*, 5325.
- (22) Meit, G. *J. Phys.: Condens. Matter* **1992**, *4*, 7521.
- (23) Pan, A. L.; Yang, H.; Liu, R.; Yu, R.; Zou, B.; Wang, Z. *J. Am. Chem. Soc.* **2005**, *127*, 15692.
- (24) Perna, G.; Pagliara, S.; Capozzi, V.; Ambrico, M.; Ligonzo, T. *Thin Solid Films* **1999**, *349*, 220.
- (25) Nogami, M.; Kato, A.; Tanaka, Y. *J. Mater. Sci.* **1993**, *28*, 4129.
- (26) Johnston, W. D. *J. Appl. Phys.* **1971**, *42*, 2731.
- (27) Hurwitz, C. E. *Appl. Phys. Lett.* **1966**, *8*, 243.
- (28) Roxlo, C. B.; Putnam, R. S.; Salour, M. M. *IEEE. J. Quantum Electron* **1982**, *QE-18*, 338.
- (29) Lu, S.; Jia, R.; Jiang, D.; Li, S. *Physica E* **2003**, *17*, 453.
- (30) Liang, Y.; Zhai, L.; Zhao, X.; Xu, D. *J. Phys. Chem. B* **2005**, *109*, 7120.
- (31) Pankove J. I. *Optical Properties in Semiconductors*; Prentice Hall: Englewood Cliffs, NJ, 1971.
- (32) Bagnall, D. M.; Chen, Y. F.; Zhu, Z.; Yao, T.; Koyama, S.; Shen, M. Y.; Goto, T. *Appl. Phys. Lett.* **1997**, *70*, 2230.